Ring Macromolecules in Topologically Restricted Environments

D. Gersappe (a) and M. Olvera de la Cruz

Department of Materials Science and Engineering, Robert R. McCormick School of Engineering and Applied Sciences, Northwestern University, Evanston, Illinois 60208 (Received 29 April 1992)

We analyze the effect of disorder on the statistics of a ring macromolecule by a computer simulation. We show how the statistics of the ring change from obeying self-avoiding to lattice animal statistics. We find a scaling relationship to characterize this crossover behavior. We further show how this problem maps onto a related study on two-dimensional vesicles with a pressure difference.

PACS numbers: 61.41.+e, 05.40.+j, 36.20.Ey

The discovery of DNA molecules in closed circular form has given rise to numerous studies on the properties of ring macromolecules. There has been a lot of work done studying the dynamics of rings in networks, which is particularly significant, as the diffusion of rings through networks is the technique of choice to help characterize these ring DNA [1,2]. The statistics of rings in random media, however, has only been postulated.

In dilute good solutions a ring obeys self-avoiding-walk statistics, i.e., the radius of gyration scaling with the molecular weight is well described by the relationship $R_g \sim N^v$, where v is the Flory exponent v = 3/(d+2). When the ring is introduced to a network, the radius of gyration is expected to be strongly affected. The network induces a net attraction between monomers of the ring polymer, as the ring cannot include any of the obstacles of the network. Therefore, if one were to increase the ring size or the concentration of impurities, a ring in a network will start obeying lattice animal or branched polymer statistics. This is in contrast to the case of linear chains where a disordered medium (annealed or quenched) does not induce a change in the chain statistics (i.e., in the exponent v), as long as the impurity concentration is below the percolation threshold [3,4].

The study of ring macromolecules in disordered networks is associated with a number of problems. In performing an analytical treatment, it is very difficult to include the constraint of the network when formulating the partition function of the ring [1]. Further, most of the computational schemes designed to study the statistics of entangled polymeric systems have been built with the purpose of studying linear chains. The topological constraint of forming a ring, in a network, introduces a number of complications, which make it rather difficult to extend the existing simulation schemes to study ring polymers. Recently, there have appeared in the literature some simulation schemes designed specifically to study end-restricted polymers, such as rings [5]. Unfortunately, these too have been built to study dilute systems of rings, and the addition of disorder into the system has yet to be addressed.

In this Letter, a new algorithm is designed to study the properties of self-avoiding ring polymers in disordered

systems via a Monte Carlo approach. We show how the properties of the ring change as the concentration of disorder is increased, and how this behavior can be described by a simple scaling relationship. We further show how the scaling behavior that we obtain through the study of rings in disorder is also present in another class of problems, namely, a two-dimensional vesicle which is subjected to a pressure difference between the interior and the exterior of the vesicle.

One of the first concerns that presents itself when one starts examining the problem of a ring in a disordered system is how one generates the ring in the first place, even before any equilibration scheme can be applied. One cannot simply start off with a random walk and attempt to close it, as then there is no way of ensuring that a network point is excluded from the interior of the ring until all the operations are performed. Computationally, this is very inefficient, and as the size of the ring or the concentration of disorder is increased, it will take a prohibitively long time just to generate the initial configuration. To overcome this we use the following scheme.

On a lattice the final form of the ring is a polygon consisting of N sides. One can subdivide this polygon into smaller polygons and continue with this subdivision until we approach a polygon whose dimensions are the size of the lattice spacing. For example, if we were to grow the ring on a square lattice, the smallest unit that the polygon is composed of would be a square of size $a \times a$, where a is the lattice spacing.

We apply this principle in reverse to grow a ring. We start off with the smallest possible unit, a "primitive cell." This primitive cell can be placed anywhere on the lattice as long as its corners do not coincide with a network point. The algorithm proceeds by choosing a side of the first cell and attaching another cell to it, such that the two cells share a common side. [This is what we refer to as a nearest-neighbor (NN) configuration. A next-nearest-neighbor (NNN) configuration would be one in which two cells share a common corner.] The perimeter of the new polygon formed is what defines the ring. Then we choose a cell at random from those which we have placed on the lattice and try to attach another cell to it in a nearest-neighbor configuration. In this way we contin-

ue attaching cells until the perimeter of the polygon formed reaches the desired value. In order to accommodate the topology of the ring polymer, when we attach these cells we have to apply three rules. The first rule is that no two cells can occupy the same site. The second rule states that a cell can have a next-nearest neighbor if and only if it and its next-nearest neighbor share a common nearest neighbor [Fig. 1(a)], and the third rule is that no cell can be attached in a configuration in which it has only two nearest neighbors on opposite faces [Fig. 1(b)].

The ring that is grown can be thought of as being composed of two types of cells, bulk cells and perimeter cells. Bulk cells have a nearest-neighbor count equal to the coordination number of the lattice. That is, they are surrounded on all sides by other cells. Perimeter cells have a nearest-neighbor count less than the coordination number of the lattice and so contribute at least one side towards the perimeter of the polygon.

Once the ring is grown inside the network, the ring is defined by a surface layer consisting of the *perimeter* cells with an underlying layer of *bulk* cells. Now, imagine that we allow cells to absorb and desorb from this surface, with equal probability. The topology of the surface has to be maintained by implementing the three rules which we have postulated earlier for the ring growth algorithm. To account for the fixed size of the ring, any event (absorption or desorption) has to conserve the perimeter of the surface. We allow for a maximum of two

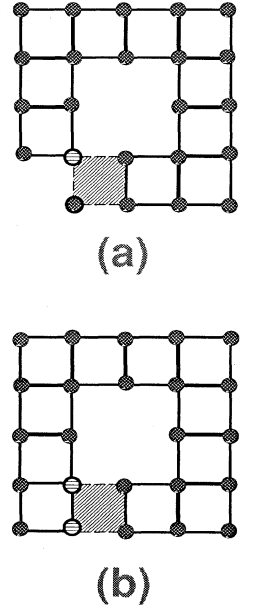


FIG. 1. The violation of the excluded volume constraint. (a) Here we have a pure *next-nearest-neighbor* contact between neighboring cells. (b) In this situation two branches of the ring coalesce. In both these situations the hatched cell is the offending cell.

events by which the perimeter of the ring is restored to its original value, i.e., if one event changes the perimeter of the ring, we allow for it to be compensated by the occurrence of a second event. (An event is defined as the absorption or desorption of a *single* cell.)

Another primary concern that arises when performing such a simulation, i.e., one in which all configurations of the ring are equally probable, is whether the algorithm is ergodic. The two types of moves that we use in our simulation have a physical analog. A one-square move can be thought of as a local perturbation of the ring, while the two-square move involves the long-range transport of monomers, in our case a kink, along the perimeter of the ring. These types of moves have also been used in simulations of self-avoiding walks by Caracciolo and Skokal [6] and have been shown to be ergodic.

In order to make sure that our algorithm recovers the correct statistics for the scaling exponent v, the simulation was run for a variety of chain lengths, in the absence of disorder. A lattice of size 64×64 was used and periodic boundary conditions were implemented. Rings of 20, 40, 60, 80, 100, 120, and 200 links were grown and equilibrated using the algorithm that we described earlier. The exponent ν which describes the radius of gyration scaling was found to be equal to 0.745 ± 0.006 , in excellent agreement with theoretical predictions as well as the previous simulations on this system [5]. Also it has been conjectured that in the absence of any disorder the area enclosed by the ring should scale with the radius of gyration of the ring as $\langle A \rangle \sim N^{2\nu}$ [7]. In our algorithm the area enclosed by the ring is simply equal to the total number of cells that comprise the ring. We found that the exponent v' that describes the scaling is equal to $2v \pm 0.005$. These seem to be strong indications that our algorithm produces equilibrium structures.

We then proceeded to calculate statistical properties of our rings in the presence of a random potential by introducing disorder into our system. Points at random were picked from an $M \times M$ integer array and then placed on a lattice of the same dimensions. Here, the advantages of using our simulation become obvious as the constraint of the disorder is simply taken care of by not allowing any corner of a *primitive cell* to coincide with an impurity point.

Before the ring growth algorithm was started, a standard cluster counting algorithm was used to identify the infinite cluster [8]. The ring was seeded on this cluster, i.e., the first primitive cell was placed on this cluster. The ring was then grown and equilibrated on this cluster. The ring was allowed $5N^2$ movements initially to equilibrate. Statistical properties of the ring were then calculated at the end of each Monte Carlo step where each step involved $5N^2$ movements of the ring. To make sure that the ring had equilibrated the movement of the center of mass of the ring was recorded, i.e., we checked to see if the ring had sampled the entire lattice. However, as the

concentration of disorder or the size of the ring was increased, the diffusion of the ring slowed down dramatically. This imposes a practical limitation on the size of the rings and the concentration of disorder that one can analyze with our algorithm.

The concentrations of disorder used were in the range of p=0.02 to p=0.12, where p is defined as the fraction of sites on the lattice that are occupied by impurities. Chains of length N=20, 40, 60, 80, 100, and 120 were used. The simulations were run for 10^5 Monte Carlo steps and the results were averaged over 5 different realizations of the disorder.

We computed the radius of gyration of the chain as a function of the concentration of disorder. One can in fact speculate, by means of a scaling argument, how the disorder would affect the statistics of the chain. We know that as the concentration of disorder is increased the ring changes from a self-avoiding walk to a lattice animal. The radius of gyration scaling, of a lattice animal, with the chain length N, goes as $R_g \sim N^{\nu_{LA}}$, where ν_{LA} is 0.64 in two dimensions [9].

We can determine the scaling factor of the radius of gyration with the concentration of disorder by use of a scaling argument. The characteristic length scales that enter the picture are R_0 , the unperturbed radius of gyration of the chain, and the length scale of the disorder, which is denoted by ξ . We can then write [10]

$$R_{\sigma}^{2}(p,N) = R_{0}^{2}\phi_{r}(R_{0}^{2}/\xi^{2}), \qquad (1)$$

where ϕ_r is a dimensionless function. In our model, the length scale ξ is simply the distance between impurities which scales with impurity concentration as $\xi \sim 1/p^{1/d}$, where d is the spatial dimension. R_0 is the unperturbed Flory radius of gyration of the chain $(R_g \sim N^{\nu})$. Therefore, $R_g^2(p,N) = R_0^2 \phi_r(pN^{2\nu})$. In the limit of $pN^{2\nu} \gg 1$ we can expand $\phi_r(x) \sim x^a$. Since in this limit we have $R_g \sim N^{\nu_{LA}}$ and $R_0 \sim N^{\nu}$, $\alpha = (\nu_{LA} - \nu)/\nu$. In Fig. 2 we plot $R_g^2/N^{2\nu}$ vs $pN^{2\nu}$. As can be seen

In Fig. 2 we plot R_g^2/N^{2V} vs pN^{2V} . As can be seen from the plot the curves for different N's the concentrations of disorder collapse to a single curve confirming our scaling argument. The value of α that was obtained from the simulation is $\alpha = -0.1217 \pm 0.02$ [11]. The value for the lattice animal exponent that we recover from our scaling plots is $v_{LA} = 0.654 \pm 0.02$. The fairly large error bars in the calculation of the exponent are a result of the small system size that we were able to use. Since subtle changes in the concentration of disorder are not picked up by this small system size, we have to use fairly large intervals when we want to compare results of different concentrations of disorder.

A very similar scaling behavior was also observed in a study of two-dimensional vesicles with a pressure difference by Leibler, Singh, and Fisher [12]. They found that the vesicle also started obeying branched polymer statistics when the pressure inside the vesicle was less than the pressure outside. They showed that the radius of gyra-

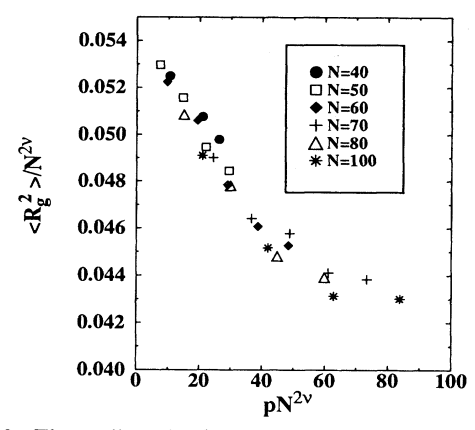


FIG. 2. The scaling plot for the radius of gyration of the ring for different ring sizes, N, and concentrations of disorder, p. As can be seen from the plot the data for the different ring sizes collapse to a single curve, confirming our scaling variable $pN^{2\nu}$.

tion could be described by a scaling law, $R_g^2 \sim N^{2\nu} \times X(\bar{p}N^{\phi\nu})$, where $\bar{p} = \Delta pa^2/k_BT$. They found that ϕ was equal to 2.13 \pm 0.17. The deviation from the expected value of 2 for ϕ was explained on the basis that they were limited by the size of the vesicles that they could use and consequently had fairly large finite-size corrections.

Leibler, Singh, and Fisher also showed that a similar scaling relationship can be derived for the area enclosed by the vesicle, i.e., $A \sim N^{2\nu_A} Y(\bar{p}N^{\phi\nu})$, where $\nu_A = \nu$ as established earlier. To complete the analogy between the problem of the vesicles we plotted the area enclosed by our ring as a function of $pN^{2\nu}$ (see Fig. 3). Again, from the plot the data collapse to a single curve.

In conclusion, we have demonstrated that the effect of introducing the topological constraint of forming a ring in

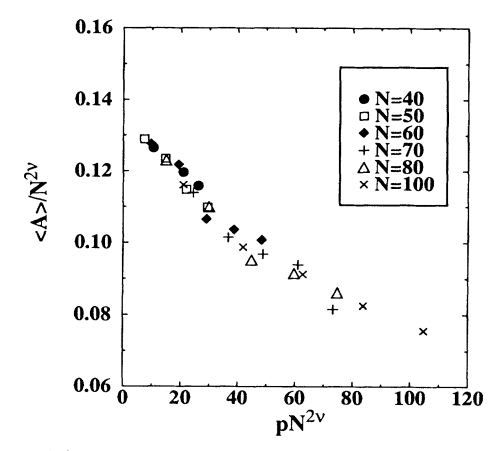


FIG. 3. The scaling plot for the area enclosed by the ring as a function of the size of the ring and the concentration of disorder. The area enclosed by the ring in our simulation is simply given by the total number of cells that comprise the ring. All the data again collapse to a single curve.

a fixed disordered network introduces a whole new series of interesting properties. The ring polymer reacts to an increase in the concentration of disorder by changing from obeying self-avoiding statistics to obeying lattice animal or branched polymer statistics. Both the radius of gyration and the area enclosed by the ring can be described by very simple scaling relationships which show the interplay between the chain length and the concentration of disorder. The similar scaling relationship found in the vesicle problem raises the interesting question as to whether the averages performed using a disorder ensemble maps onto the pressure ensemble. In our problem the analog of the scaled pressure difference used by Leibler, Singh, and Fisher is p, the concentration of impurities.

While the algorithm we have outlined in this paper has been specific to a square lattice, it can be easily extended to other lattices with the proper choice of a *primitive cell*. For example, in a triangular lattice one would start with a rhombus, composed of two equilateral triangles and then proceed in the same manner as with the square lattice. The extension of this algorithm to the third dimension is also possible. Since the algorithm generates closed surfaces at each step, the inclusion of the third dimension will be straightforward as knots cannot be generated via this algorithm.

We thank J. M. Deutsch, B. Duplantier, and K. A. Dawson for useful discussions. M.O. wishes to acknowledge financial support from the Lucile and David Packard Foundation. This work was supported in part by NSF Grant No. DMR 9057764 and by a grant from the National Institutes of Health.

- (a) Present address: Department of Materials Science and Engineering, University of Pittsburgh, Pittsburgh, PA 15261.
- [1] M. E. Cates and J. M. Deutsch, J. Phys. (Paris) 47, 2121 (1986).
- [2] M. Rubenstein, Phys. Rev. Lett. 57, 3023 (1986).
- [3] S. B. Lee and H. Nakanishi, Phys. Rev. Lett. 61, 2022 (1988).
- [4] D. Gersappe, J. M. Deutsch, and M. O. de la Cruz, Phys. Rev. Lett. 66, 731 (1991).
- [5] M. Murat and T. Witten, Macromolecules 23, 23 (1990);
 J. Reiter, Macromolecules 23, 3811 (1990); A. Romero,
 J. Phys. I (France) 2, 15 (1992).
- [6] S. Caracciolo and A. Skokal, J. Phys. A 19, L797 (1986).
- [7] M. E. Fisher, Physica (Amsterdam) 38D, 112 (1989).
- [8] K. Binder and D. W. Heermann, Monte Carlo Simulation in Statistical Physics: An Introduction (Springer-Verlag, Berlin, 1988).
- [9] B. Derrida and D. Stauffer, J. Phys. (Paris) 46, 1623 (1985).
- [10] P. de Gennes, Scaling Concepts in Polymer Physics (Cornell Univ. Press, Ithaca, 1979).
- [11] In calculating the exponent α we did not use points which corresponded to the lowest and highest values of the porosity for each individual chain. This was done as at low concentrations of disorder the scaling argument is no longer valid, and at higher concentrations the rings take a much longer time to equilibrate, resulting in poorer statistics.
- [12] S. Leibler, R. Singh, and M. E. Fisher, Phys. Rev. Lett. 59, 1989 (1987).